ARTICLE
Journal of Cellular Biochemistry 112:1787–1794 (2011)

Journal of Cellular Biochemistry

HSP75 Protects Against Cardiac Hypertrophy and Fibrosis

Yan Zhang,[1,2] Ding-Sheng Jiang,[2] Ling Yan,[1,2] Kuo-Ju Cheng,[2] Zhou-Yan Bian,[1,2] and Guo-Sheng Lin[1,2*]

[1]*Department of Cardiology, Renmin Hospital of Wuhan University, Wuhan 430060, PR China*
[2]*Cardiovascular Research Institute of Wuhan University, Wuhan 430060, PR China*

ABSTRACT

Cardiac hypertrophy, a major determinant of heart failure, is associated with heat shock proteins (HSPs). HSP75 has been reported to protect against environmental stresses; however, its roles in cardiac hypertrophy remain unclear. Here, we generated cardiac-specific inducible HSP75 transgenic mice (TG) and cardiac hypertrophy was developed at 4 weeks after aortic banding in TG mice and wild-type littermates. The results revealed that overexpression of HSP75 prevented cardiac hypertrophy and fibrosis as assessed by heart weight/body weight ratio, heart weight/tibia length ratio, echocardiographic and hemodynamic parameters, cardiomyocyte width, left ventricular collagen volume, and gene expression of hypertrophic markers. Further studies showed that overexpression of HSP75 inhibited the activation of TAK/P38, JNK, and AKT signaling pathways. Thus, HSP75 likely reduces the hypertrophy and fibrosis induced by pressure overload through blocking TAK/P38, JNK, and AKT signaling pathways. J. Cell. Biochem. 112: 1787–1794, 2011.

KEY WORDS: HSP75; HYPERTROPHY; FIBROSIS; TAK; JNK1/2; AKT

Cardiac hypertrophy is a common response of the heart to a variety of pathological stimuli, such as hypertension, ischemia, pressure overload, and sarcomeric gene mutation, and it is frequently characterized by myocyte hypertrophy, disarray, and interstitial fibrosis [Ho et al., 2010; Jefferies and Towbin, 2010]. Although pathological hypertrophy of the myocardium is temporarily compensatory, prolonged hypertrophy may result in ventricular arrhythmias, heart failure, and subsequent cardiovascular mortality [Lakdawala and Givertz, 2010]. Therefore, it is very important to elucidate the underlying mechanism of cardiac hypertrophy. A growing body of evidence indicates that heat shock proteins (HSPs) are involved in cardiac hypertrophy [Hayashi et al., 2006; Willis and Patterson, 2010]. HSPs are a family of proteins that become active following increases in temperature and other environmental stresses, and they are well known to play roles in signal transduction, protein folding, translocation, degradation, and the assembly of intracellular proteins, which may protect against various environmental challenges [Richter et al., 2010]. The activities of several members of the HSP family, such as HSP56, HSP70, HSP 90, and HSP20, have been shown to be induced by hypertrophic stimuli and regulate cardiac hypertrophy via different mechanisms [Fan et al., 2006; Ruiz-Hurtado et al., 2007; Kee et al., 2008; Cai et al., 2010]. For example, the cardioprotective effect of the anti-HSP70 antibody was indicated by attenuating pro-hypertrophy signal the mitogen-activated protein kinases (MAPK) P38 and ERK [Cai et al., 2010]. Cardiac hypertrophy and fibrosis are dependent on many signaling pathways. These important signaling pathways include the MAPK pathway and the phosphatidylinositol 3-kinase (PI3K)/Akt pathway which directly modify transcriptional regulatory factors promoting alterations in cardiac gene expression and result in cardiac hypertrophy and fibrosis [Heineke and Molkentin, 2006]. So a better understanding of the roles of HSPs and their mechanisms in cardiac hypertrophy may lead to novel strategies for suppressing cardiac hypertrophy and preventing the transition to heart failure.

HSP75, which is also called tumor necrosis factor-associated protein 1 (TRAP-1), is a mitochondrially localized member of the HSP90 family. HSP75 is induced by various environmental stresses, such as glucose deprivation, oxidative injury, and ultraviolet A irradiation, and acts as a mitochondrial chaperone involved in maintaining mitochondrial function and regulating cell apoptosis [Hua et al., 2007; Pridgeon et al., 2007; Voloboueva et al., 2008; Landriscina et al., 2010]. The overexpression of HSP75 has been shown to protect against mitochondrial dysfunction, oxidative stress, and ischemic injury-induced apoptosis in brain cells and cardiac myocytes [Voloboueva et al., 2008; Xu et al., 2009]; however, the effects of HSP75 on cardiac hypertrophy and the related signaling mechanisms therein still remain unclear. In the present study, we used HSP75-transgenic mice to investigate the role of HSP75 in pressure overload-induced cardiac hypertrophy

*Correspondence to: Dr. Guo-Sheng Lin, MD, PhD, Department of Cardiology of Renmin Hospital of Wuhan University, JieFang Road 238, Wuhan 430060, PR China. E-mail: lgs1027_phb@163.com
Received 29 December 2010; Accepted 25 February 2011 • DOI 10.1002/jcb.23091 • © 2011 Wiley-Liss, Inc.
Published online 4 March 2011 in Wiley Online Library (wileyonlinelibrary.com).

and its related molecular mechanisms. We show, for the first time, that HSP75 functions as a novel anti-hypertrophic regulator by blocking the TAK/P38, JNK, and AKT pathways.

MATERIALS AND METHODS

CARDIAC-SPECIFIC HSP75 TRANSGENIC MICE

All of the protocols used in this study were approved by the Animal Care and Use Committee of Renmin Hospital, Wuhan University. A human HSP75 cDNA construct that contained full-length human HSP75 cDNA was cloned downstream of the human cardiac α-myosin heavy chain (α-MHC) promoter. Transgenic mice were produced by microinjecting the α-MHC-HSP75 construct into fertilized mouse embryos (C57 background). Four independent transgenic lines were established and studied. Transgenic mice were identified by PCR analysis of tail genomic DNA. The primers were as follows: 5′-TGCGAGATGTGGTAACG AAG-3′ and 5′-GCATGAA-CAGGCCGTAATCT-3′. The expected PCR band size was 537 bp in length. The expression levels were analyzed as pairs of α-MHC-HSP75 (TG) and littermate nontransgenic wild-type (WT) male mice ranging in age from 7 to 8 weeks.

ANIMAL MODELS, ECHOCARDIOGRAPHY, AND HEMODYNAMIC MEASUREMENTS

Aortic banding (AB) was performed as described previously [Bian et al., 2010; Li et al., 2010]. Sham-operated mice underwent the same procedure without constriction. Four weeks after the AB operation, echocardiography was performed in order to test the morphology and function of the mice using Mylab30CV (ESAOTE). The left ventricular (LV) situations was assessed in parasternal short-axis views at a frame rate of 50 Hz. End-systole and end-diastole phases were defined as the phases with the smallest and largest LV areas, respectively. Left ventricular end-systolic diameter (LVESD) and left ventricular end-diastolic diameter (LVEDD) were measured from the M-mode tracing with a sweep speed of 10 mm/s at the mid-papillary muscle level. The LVED dimension (LVEDD) and LVES dimension (LVESD) were measured using M-mode tracing with a sweep speed of 10 mm/s at the papillary muscle level. Blood pressure was recorded via a microtip catheter transducer (SPR-839, Millar Instruments) that was inserted into the right carotid artery and advanced into the left ventricle for hemodynamic measurements. The hearts and lungs of the sacrificed mice were dissected and weighed to compare the heart weight/body weight (HW/BW, mg/g), lung weight/body weight (LW/BW, mg/g), and heart weight/tibia length (HW/TL, mg/cm) ratios.

HISTOLOGICAL ANALYSIS

The hearts were washed with 10% potassium chloride, placed in 10% formalin, transversely cut close to the apex in order to visualize the left and right ventricles, and paraffin-embedded. Several sections of heart (5 μm thick) were prepared and stained with hematoxylin and eosin (HE) for histopathological analysis or picrosirius red (PSR) for collagen deposition analysis and then visualized by light microscopy. To measure the myocyte cross-sectional areas (CSA), the sections were stained with HE. A single myocyte was measured using an image-based quantitative digital analysis system (Image Pro-Plus, version 6.0). The outlines of 100–200 myocytes were traced in each group.

WESTERN BLOTTING AND QUANTITATIVE REAL-TIME PCR

For Western blotting analysis, the cardiac tissues were lysed via a RIPA lysis buffer. A BCA protein assay kit (Themo, 23227) was used to measure protein concentration by ELISA (Synergy HT, Bio-tek). Fifty micrograms of the tissue lysate were separated on 4–12% Bis–Tris NuPage gels (Invitrogen, NP0321BOX), and the proteins were then transferred onto Immobilon-FL transfer membranes (Millipore, IPFL00010). The primary antibodies were: p-AKT (Cell Signaling Technology, 4060L), T-AKT (Cell Signaling Technology, 4691L), p-ERK (Cell Signaling Technology, 4370L), T-ERK (Cell Signaling Technology, 4695), p-P38 (Cell Signaling Technology, 4511L), T-P38 (Cell Signaling Technology, 9212L), p-JNK (Cell Signaling Technology, 4668S), T-JNK (Cell Signaling Technology, 9258), p-TAK (Cell Signaling Technology, 9339), T-TAK (Cell Signaling Technology, 4505), HSP75 (Abcam, human: ab3287, mouse: ab2799), and GAPDH (Bioworld, MB001). The secondary antibodies were either goat anti-rabbit (LI-COR, 926–32211) or mouse (LI-COR, 926–32210) immunoglobulin G (IgG). The protein bands were detected using a two-color infrared imaging system (Odyssey, Li-COR). The specific protein expression levels were normalized to the glyceraldehyde-3-phosphate dehydrogenase (GAPDH) protein in order to evaluate the total cell lysate and cytosolic proteins.

For quantitative real-time PCR, the total RNAs were extracted from frozen mouse tissues using TRIzol (Invitrogen, 15596–026), and their yields and purities were spectrophotometrically estimated using the A260/A280 and A230/260 ratios via a SmartSpec Plus Spectrophotometer (Bio-Rad). The RNA (2 μg) was reverse-transcribed into cDNA using oligo (dT18) primers using the Transcriptor First Strand cDNA Synthesis Kit (Roche, 04896866001). We quantified the PCR amplifications using a LightCycler 480 SYBR Green 1 Master Mix (Roche, 04707516001) and the following primers were used: mouse *ANP* 5′-ACCTGCTAGACCACCTGGAG-3′ (forward) and 5′-CCTTGGCTGTTATCTTCGGTAC CGG-3′ (reverse); mouse *MYH6* 5′-AGCTGACAGGGGCCATCAT-3′ (forward) and 5′-ACATACTCGTTCCCCACCTTC-3′ (reverse); mouse *MYH7* 5′-TTCAT-CCGAATCCATTTT GGGG-3′ (forward) and 5′-GCATAATCGTAGGG-GTTGTTGG-3′ (reverse); mouse *TGF-β* 5′-TCGACATGGATCAGTT-TATGCG-3′(forward) and 5′-CCCTGGTACTGTTGTAGATGG A-3′(reverse); mouse *CTGF* 5′-TGACCCCTGCGACCCACA-3′ (forward) and 5′-TACACC GACCCACCGAAGA CACAG-3′ (reverse); mouse *Collagen I* 5′-AGGCTTCAGTGGTTT GGATG-3′ (forward) and 5′-CACCAACAGCACCATCGTTA-3′ (reverse); mouse *Collagen III* 5′-CCCAACCCAGAGATCCCATT-3′(forward) and 5′-GAAGCACAG-GAGCAGGTGTA GA-3′ (reverse). Those programs were performed, recorded, and analyzed by using the LightCycler 480 (Roche). The results were normalized against GAPDH gene expression.

STATISTICAL ANALYSIS

Data were expressed as means ± SEM. Differences among groups were tested by one-way ANOVA followed by post hoc LSD test or Tamhane's T2 test. $P < 0.05$ was considered to be significantly different.

RESULTS

HSP75 EXPRESSION IN A PRESSURE OVERLOAD-INDUCED HYPERTROPHY MODEL AND CHARACTERIZATION OF CARDIAC-SPECIFIC HSP75-TRANSGENIC MICE

Although HSP75 expression is low in normal mice, we found that HSP75 levels in the murine heart were gradually elevated from 1 day to 4 weeks after the AB operation; however, HSP75 expression was markedly decreased 8 weeks after the AB operation (Fig. 1A). Thus, HSP75 expression is regulated during pressure overload-induced left ventricular remodeling.

To examine the functional consequences of increased HSP75 expression in the heart, we established four independent cardiac-specific TG strains that has a origin of human HSP75 mRNA. Western blotting analysis was used to compare the increased levels of HSP75 protein expression in TG hearts across the different founder lines. The levels of transgene expression varied across the different founders, as shown in Figure 1B. One of the TG lines (TG3) had the highest expression level of the transgene transcript in the heart, and TG1 had a moderate level of transgene expression in the heart; however, the other two TG lineages (TG2 and TG4) exhibited low levels of transgene expression in the heart in comparison to those in the WT hearts (Fig. 1B).

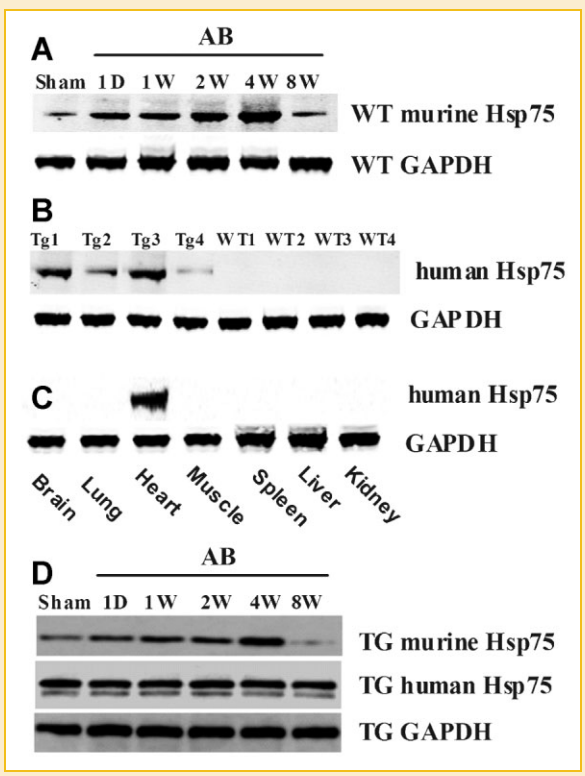

Fig. 1. The expression of HSP75 in a pressure overload-induced hypertrophy model and the characterization of cardiac-specific HSP75 transgenic mice. A: HSP75 expression after AB. Representative protein levels of murine HSP75 in WT heart tissues after AB at time points indicated by Western blot analysis. B: Human HSP75 protein in the heart tissues from four lines of both TG and WT mice. C: Characterization of human HSP75-TG mice. HSP75 protein expression in different tissues. D: Representative protein levels of murine and human HSP75 in TG heart tissues after AB at time points indicated by Western blot analysis.

Because the transgene in HSP75-TG mice has a human mRNA 75 origin, we selected a transgenic mouse line (TG3) and used Western blotting to analyze HSP75 protein levels in various tissues using a primary antibody specific to the human HSP75 sequence. Thus, we were able to distinguish the HSP75 transgene from endogenous mouse HSP75. The results indicate that HSP75 overexpression was restricted to the heart and was not detectable in other tissues, such as brain, lung, muscle, spleen, liver, and kidney (Fig. 1C). And we found that murine HSP75 levels in the TG murine heart were also gradually elevated from 1 day to 4 weeks after the AB operation; however, human HSP75 expression maintained the same levels after the AB operation (Fig. 1D).

OVEREXPRESSION OF HSP75 AMELIORATES AB-INDUCED CARDIAC HYPERTROPHY

To investigate the effect of elevated cardiac HSP75 expression on the development of cardiac hypertrophy, HSP75-TG mice and WT mice were subjected to either chronic AB-induced pressure overload or sham surgery (as a control procedure). After 4 weeks, cardiac hypertrophy and function were assessed by echocardiographic analyses and pressure–volume (PV) loop analysis, including fractional shortening (FS), LVEDD, LVESD, interventricular septal dimension (IVSD), left ventriculus posterior wall dimension (LVPWD), ejection fraction (EF), systolic blood pressure (SBP), dp/dt max, and dp/dt min, in all of the mice of all four groups. No significant changes were observed between the sham-operated HSP75-TG and WT mice; however, the results indicate that the WT mice subjected to AB exhibited pathological hypertrophy and cardiac dysfunction, unlike the WT sham mice. Furthermore, the HSP75-TG mice that were subjected to AB exhibited fewer indications of cardiac dysfunction (including increases in FS, EF, dp/dt max, and dp/dt min and decreases in LVEDD, LVESD, IVSD, and LVPWD) than the WT mice that were subjected to AB (Fig. 2A,B). Therefore, the overexpression of HSP75 was able to prevent ventricular dysfunction by reversing hypertrophic remodeling.

As expected, all WT mice subjected to AB exhibited the classical increases in HW and size in comparison to the sham control group at 4 weeks postoperation. In contrast, the inhibitory effect of HSP75 overexpression on cardiac hypertrophy in hearts subjected to AB was confirmed by the direct observation of the gross morphology of the heart. No significant changes were observed in the sham-operated TG or WT mice (Fig. 2C,D). The augmentation in cardiac myocyte size observed after HE staining in the TG mice was also markedly attenuated in comparison to that in WT mice 4 weeks postoperation. The TG mice that had been subjected to AB exhibited an intriguing diminution in cardiac hypertrophy, as measured by the HW/BW, LW/BW, and HW/TL ratios (Fig. 2D) and the cardiomyocyte CSA (Fig. 3E).

To investigate whether the overexpression of HSP75 affected the mRNA expression levels of cardiac hypertrophy markers, real-time PCR was performed to analyze atrial natriuretic peptide (*ANP*), *Myh6*, and *Myh7*. In comparison to WT mice, the overexpression of HSP75 attenuated the pressure overload-induced changes in the expression of hypertrophic markers *ANP*, *Myh7*, and the induction

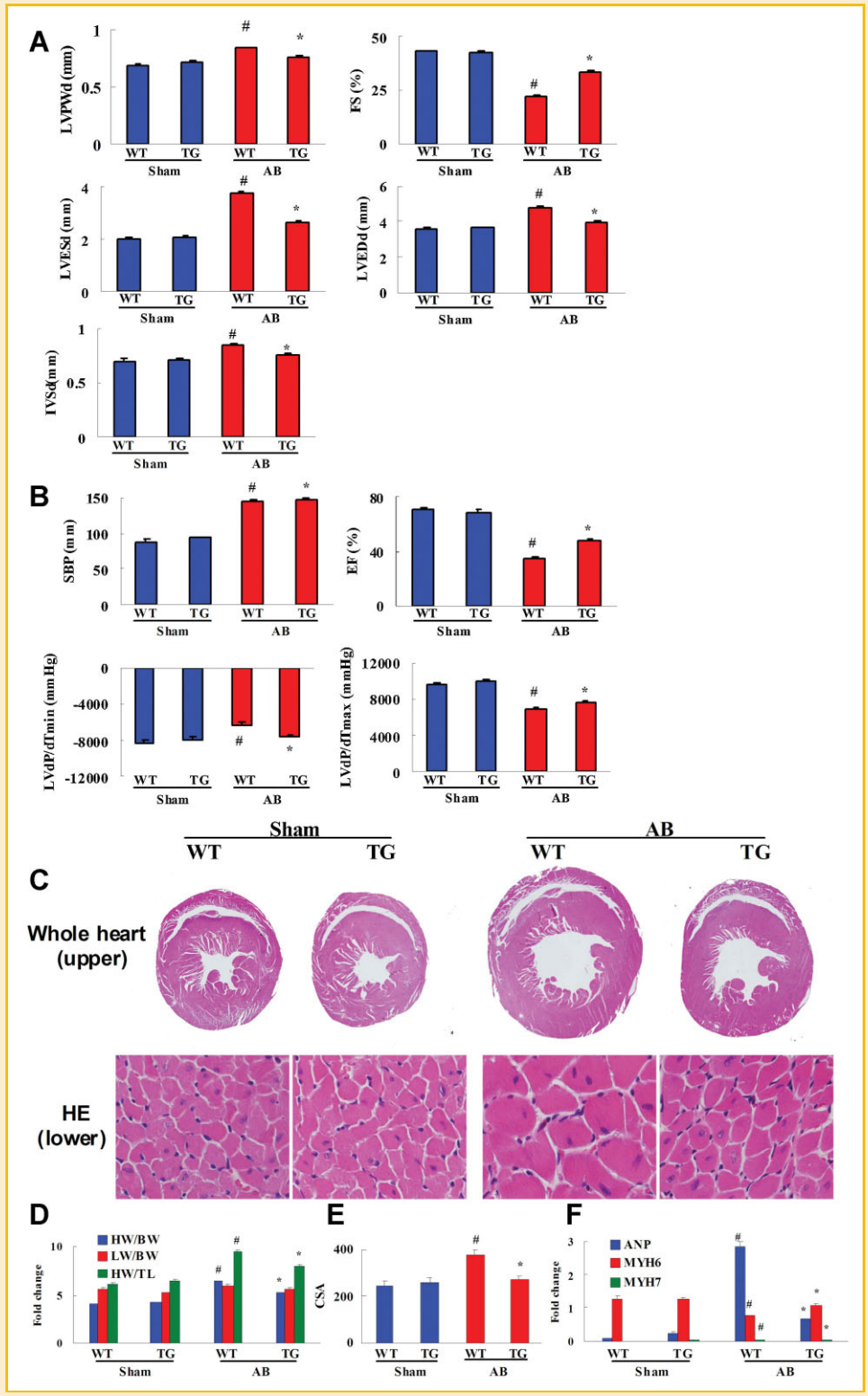

Fig. 2. The overexpression of HSP75 inhibits cardiac hypertrophy. The results of echocardiography (A) and PV (B) experiments on sham- and AB-treated mice 4 weeks after surgery (n = 12 mice per group). The whole hearts (C, top) and HE staining (C, bottom) of sham- and AB-treated mice 4 weeks after surgery. The statistical results of the HW/BW, LW/BW, and HW/TL ratios (D), and myocyte cross-sectional areas (E) 4 weeks after surgery (n = 8 mice per group). (F) The mRNA expression levels of ANP, MYH6, and MYH7 (n = 4) by real-time PCR analysis. #$P < 0.05$ versus WT/sham. *$P < 0.05$ versus WT after AB.

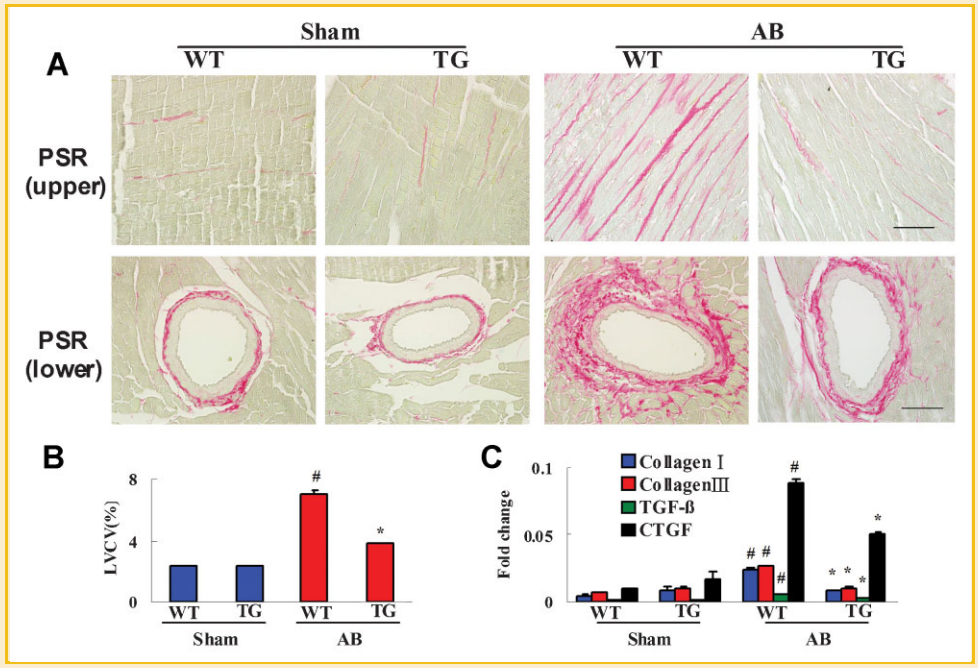

Fig. 3. The overexpression of HSP75 inhibits cardiac fibrosis. A: PSR was performed in order to show the AB-induced left ventricular collagen volume (LVCV) in the four groups of animals (scale bar: 10 μm). B: The statistical results of the fibrotic areas of the histological sections (n = 8 mice per group). C: The mRNA expression levels of the fibrotic markers by real-time PCR analysis (n = 4). #$P < 0.05$ versus WT/sham. *$P < 0.05$ versus WT after AB.

of hypertrophic markers *Myh6* was increased in TG mice response to AB compared to that in WT in Figure 2F; however, the sham-operated TG mice exhibited no significant changes in the expression levels of the *ANP*, *Myh6*, and *Myh7* genes in comparison to the control mice (Fig. 2F). These findings indicate that the overexpression of HSP75 prevents the development of cardiac hypertrophy.

OVEREXPRESSION OF HSP75 RESCUES AB-INDUCED CARDIAC FIBROSIS

Mounting evidence has demonstrated that fibrosis is an important pathophysiological feature of the development of cardiac hypertrophy. To explore whether the overexpression of HSP75 can suppress the fibrotic response to cardiac hypertrophy, we investigated the extent of interstitial fibrosis via PSR staining and light microscopy. No significant difference in fibrosis was observed between the WT and TG mice 4 weeks after the sham operation. In contrast to normal hearts with little fibrotic tissue, marked interstitial fibrosis was detected in the WT mice that were subjected to AB; however, the augmentation of the left ventricular collagen volume was remarkably attenuated in the TG mice that had been subjected to AB (Fig. 3A,B).

To further elucidate the molecular mechanisms that underlie the effect of HSP75 overexpression on collagen synthesis, the mRNA expression levels of known mediators of fibrosis, including connective tissue growth factor (*CTGF*, a key mediator of extracellular matrix deposition), transforming growth factor (*TGF-β*), and *collagens I* and *III*, were analyzed. Four weeks after the sham operation, the expression levels of these mediators were similar in the TG and WT mice, but their levels were almost threefold greater in the WT mice that had been subjected to AB than in the sham mice; however, all of these increases were blunted in the TG mice that had been subjected to AB in comparison to the WT mice that had been subjected to AB (Fig. 3C).

OVEREXPRESSION OF HSP75 REGULATES MAPK- AND AKT-RELATED SIGNALING

To explore the molecular mechanisms through which the overexpression of HSP75 impairs cardiac hypertrophy and fibrosis in response to hypertrophic stimuli, we further assessed the effects of HSP75 overexpression on related signaling pathways (e.g., the MAPK pathways). Our data indicate that TAK, ERK1/2, JNK1/2, and p38 were significantly phosphorylated in mice that had been subjected to AB; however, the phosphorylations of TAK, JNK1/2, and P38 were almost completely blocked in the TG mice after AB, whereas ERK1/2 was not significantly affected. The dramatic inhibitions of TAK, JNK1/2, and P38 activation in TG mice were independent of the reduction in the total TAK, JNK1/2, and P38 protein levels, respectively (Fig. 4A,B). Collectively, these data suggest that overexpression of HSP75 reduces the activation of TAK, P38, and JNK1/2 signaling, although it has no effect on ERK1/2 activation in hearts that have been subjected to AB.

To further determine whether overexpression of HSP75 also blocks the AKT pathway in response to hypertrophic stimuli, we examined the phosphorylation of AKT. Our results reveal significant AKT phosphorylation after AB in comparison to the sham group, and such changes were inhibited in TG mice (Fig. 4A,B). Taken together, our findings imply that the TAK/MAPK pathway and AKT

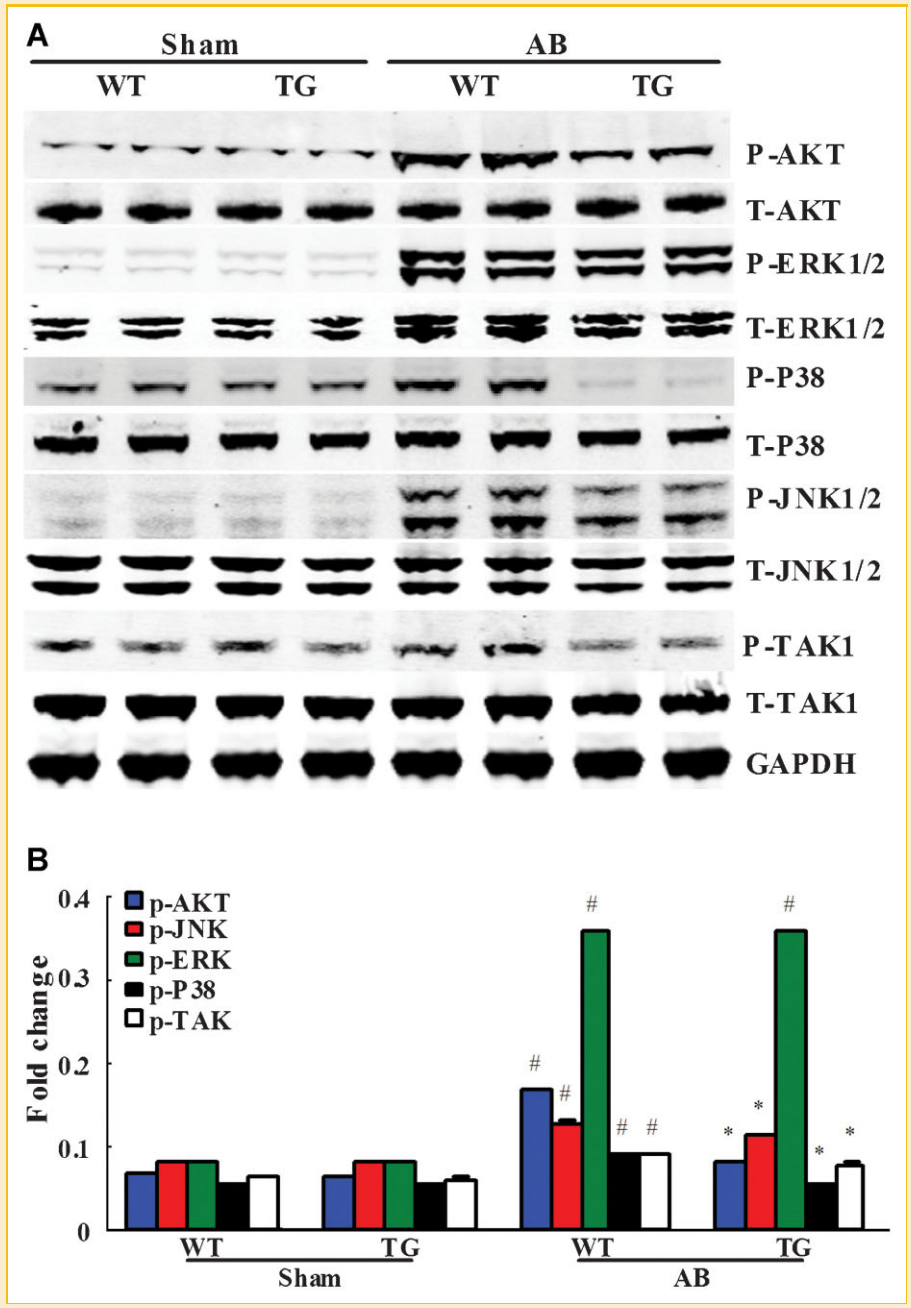

Fig. 4. The effects of HSP75 overexpression on MAPK and AKT signaling. A: The phosphorylation levels of AKT, ERK1/2, JNK1/2, p38, and TAK in AB-treated mice. AB-induced phosphorylations of AKT, JNK1/2, p38, and TAK were almost completely impaired in TG mice, as determined by Western blot analysis. GAPDH was used as a loading control. B: The quantification of the protein bands ($n = 4$). #$P < 0.05$ versus WT/sham. *$P < 0.05$ versus WT after AB.

signaling play important roles in HSP75 overexpression-mediated inhibition of cardiac hypertrophy and fibrosis.

DISCUSSION

As a member of the highly conserved HSP family, which is involved in various host defense mechanisms against environmental stresses [Richter et al., 2010], HSP75 may also protect against the pathological development of cardiovascular diseases; however, to date, its function in cardiac hypertrophy remains unclear. In the present study, we investigated the role of HSP75 in cardiac hypertrophy using cardiac-specific, HSP75-overexpressing transgenic mice. HSP75 overexpression profoundly attenuated pressure overload-induced cardiac hypertrophy and fibrosis. Further analyses of the signaling events indicate that cardioprotection by HSP75 is mediated by the interruption of TAK/P38, JNK, and AKT signaling. To our knowledge, this is the first report to demonstrate a crucial role for HSP75 in the regulation of cardiac hypertrophy and fibrosis.

HSP75, which is a member of the HSP90 family, localizes to mitochondria and functions as a mitochondrial chaperone involved in maintaining mitochondrial function and regulating cell apoptosis. There is increasing evidence for the involvement of HSP75 in responses to various environmental stresses, including glucose deprivation, oxidative injury, and ultraviolet A irradiation [Hua et al., 2007; Pridgeon et al., 2007; Volobouéva et al., 2008; Xu et al., 2009]. The capability of hypertrophic stress to induce HSP75 expression was tested for the first time in the present study. In response to pressure overload, HSP75 expression increased during adaptive hypertrophy and markedly decreased during maladaptive cardiac remodeling, suggesting that HSP75 is involved in the defense against hypertrophic stress. To further examine the potential function of HSP75 in cardiac hypertrophy, we generated cardiac-specific HSP75-transgenic mice. As predicted, HSP75-TG mice exhibited a significant attenuation of hypertrophy 4 weeks after AB in comparison to WT mice, as evidenced by cardiac mass and function and histological and molecular analyses. Moreover, HSP75 blocks cardiac fibrosis and attenuates the pressure overload-induced expression of several fibrotic mediators. Together, these findings indicate that HSP75 plays a critical role in preventing cardiac hypertrophy and fibrosis. Our results are consistent with previous studies showing that other members of the HSP family, such as HSP90, HSP70, HSP20, and αB-crystallin, suppress the cardiac hypertrophy induced by angiotensin II, isoproterenol stimulation, or pressure overload [Hayashi et al., 2006; Willis and Patterson, 2010]. These findings support the idea that the HSP family may be involved in mechanisms that protect against pathological cardiac remodeling and may be effective therapeutic candidates for cardiac hypertrophy and heart failure.

The molecular mechanism by which HSP75 mediates its anti-hypertrophic and anti-fibrotic effects remains largely unclear. Mounting evidence has suggested that the MAPK and AKT signaling pathways play important roles in cardiac hypertrophy and fibrosis [Lorenz et al., 2009; Rose et al., 2010]. Therefore, the inhibitory effects of HSP75 on cardiac remodeling were examined in the context of MAPK and AKT signaling. Our results indicate that the pressure overload-induced increases in the TAK, P38, JNK, and AKT phosphorylation levels were almost completely blocked in HSP75-TG hearts. The phosphorylation of ERK1/2 was not significantly affected by HSP75 overexpression. Therefore, the blockade of TAK/P38, JNK, and AKT signaling dictates the cardioprotective effects of HSP75. In agreement with our findings, the development of cardiac hypertrophy in Hsp70-KO mice results from the activation of the JNK and p38-MAPK pathways [Kim et al., 2006]. Recent studies have demonstrated that the overexpression of Hsp75 protects against mitochondrial dysfunction, oxidative stress, and ischemic injury-induced apoptosis in brain cells and cardiac myocytes. Given the important pro-hypertrophic effects of oxidative stress and apoptosis [Hua et al., 2007; Xu et al., 2009], we cannot exclude the possibility that these mechanisms underlie the anti-hypertrophic role of HSP75. Further experiments are needed to investigate this hypothesis.

In summary, our present work demonstrates, for the first time, that HSP75 inhibits cardiac hypertrophy and fibrosis by blocking the TAK/P38, JNK, and AKT signaling pathways. Our study provides insight into the pathogenesis of cardiac hypertrophy and may have significant implications for the development of novel strategies that block cardiac remodeling and the progression to heart failure by targeting HSP75.

REFERENCES

Bian ZY, Huang H, Jiang H, Shen DF, Yan L, Zhu LH, Wang L, Cao F, Liu C, Tang QZ, Li HL. 2010. LIM and cysteine-rich domains 1 regulates cardiac hypertrophy by targeting calcineurin/nuclear factor of activated T cells signaling. Hypertension 55:257–263.

Cai WF, Zhang XW, Yan HM, Ma YG, Wang XX, Yan J, Xin BM, Lv XX, Wang QQ, Wang ZY, Yang HZ, Hu ZW. 2010. Intracellular or extracellular heat shock protein 70 differentially regulates cardiac remodeling in pressure overload mice. Cardiovasc Res 88:140–149.

Fan GC, Yuan Q, Song G, Wang Y, Chen G, Qian J, Zhou X, Lee YJ, Ashraf M, Kranias EG. 2006. Small heat-shock protein Hsp20 attenuates beta-agonist-mediated cardiac remodeling through apoptosis signal-regulating kinase 1. Circ Res 99:1233–1242.

Hayashi M, Imanaka-Yoshida K, Yoshida T, Wood M, Fearns C, Tatake RJ, Lee JD. 2006. A crucial role of mitochondrial Hsp40 in preventing dilated cardiomyopathy. Nat Med 12:128–132.

Heineke J, Molkentin JD. 2006. Regulation of cardiac hypertrophy by intracellular signalling pathways. Nat Rev Mol Cell Biol 7:589–600.

Ho CY, López B, Coelho-Filho OR, Lakdawala NK, Cirino AL, Jarolim P, Kwong R, González A, Colan SD, Seidman JG, Díez J, Seidman CE. 2010. Myocardial fibrosis as an early manifestation of hypertrophic cardiomyopathy. N Engl J Med 363:552–563.

Hua G, Zhang Q, Fan Z. 2007. Heat shock protein 75 (TRAP1) antagonizes reactive oxygen species generation and protects cells from granzyme M-mediated apoptosis. J Biol Chem 282:20553–20560.

Jefferies JL, Towbin JA. 2010. Dilated cardiomyopathy. Lancet 375:752–762.

Kee HJ, Eom GH, Joung H, Shin S, Kim JR, Cho YK, Choe N, Sim BW, Jo D, Jeong MH, Kim KK, Seo JS, Kook H. 2008. Activation of histone deacetylase 2 by inducible heat shock protein 70 in cardiac hypertrophy. Circ Res 103: 1259–1269.

Kim YK, Suarez J, Hu Y, McDonough PM, Boer C, Dix DJ, Dillmann WH. 2006. Deletion of the inducible 70-kDa heat shock protein genes in mice impairs cardiac contractile function and calcium handling associated with hypertrophy. Circulation 113:2589–2597.

Lakdawala NK, Givertz MM. 2010. Dilated cardiomyopathy with conduction disease and arrhythmia. Circulation 122:527–534.

Landriscina M, Laudiero G, Maddalena F, Amoroso MR, Piscazzi A, Cozzolino F, Monti M, Garbi C, Fersini A, Pucci P, Esposito F. 2010. Mitochondrial chaperone Trap1 and the calcium binding protein Sorcin interact and protect cells against apoptosis induced by antiblastic agents. Cancer Res 70:6577–6586.

Li H, He C, Feng J, Zhang Y, Tang Q, Bian Z, Bai X, Zhou H, Jiang H, Heximer SP, Qin M, Huang H, Liu PP, Huang C. 2010. Regulator of G protein signaling 5 protects against cardiac hypertrophy and fibrosis during biomechanical stress of pressure overload. Proc Natl Acad Sci USA 107:13818–13823.

Lorenz K, Schmitt JP, Schmitteckert EM, Lohse MJ. 2009. A new type of ERK1/2 autophosphorylation causes cardiac hypertrophy. Nat Med 15: 75–83.

Pridgeon JW, Olzmann JA, Chin LS, Li L. 2007. PINK1 protects against oxidative stress by phosphorylating mitochondrial chaperone TRAP1. PLoS Biol 5:e172.

Richter K, Haslbeck M, Buchner J. 2010. The heat shock response: Life on the verge of death. Mol Cell 40:253–266.

Rose BA, Force T, Wang Y. 2010. Mitogen-activated protein kinase signaling in the heart: Angels versus demons in a heart-breaking tale. Physiol Rev 90:1507–1546.

Ruiz-Hurtado G, Fernández-Velasco M, Mourelle M, Delgado C. 2007. LA419, a novel nitric oxide donor, prevents pathological cardiac remodeling in pressure-overloaded rats via endothelial nitric oxide synthase pathway regulation. Hypertension 50:1049–1056.

Voloboueva LA, Duan M, Ouyang Y, Emery JF, Stoy C, Giffard RG. 2008. Overexpression of mitochondrial Hsp70/Hsp75 protects astrocytes against ischemic injury in vitro. J Cereb Blood Flow Metab 28:1009–1016.

Willis MS, Patterson C. 2010. Hold me tight: Role of the heat shock protein family of chaperones in cardiac disease. Circulation 122:1740–1751.

Xu L, Voloboueva LA, Ouyang Y, Emery JF, Giffard RG. 2009. Overexpression of mitochondrial Hsp70/Hsp75 in rat brain protects mitochondria, reduces oxidative stress, and protects from focal ischemia. J Cereb Blood Flow Metab 29:365–374.